International Journal of Thin Films Science and Technology

http://dx.doi.org/10.18576/ijtfst/080107

Temperature Dependence on Optical Properties of Sr Doped $BaTiO_3$ Thin films by Vacuum Evaporation Method

R. Sengodan [1], R. Kannan [1], R. Balamurugan [1] and B. Chandra Shekar[2]*

[1]Department of Physics, Kumaraguru College of Technology, Coimbatore – 641049,Tamil Nadu, India.
[2]Departments of Physics, Kongunadu Arts and Science College, G.N- Mills, Coimbatore – 641029, Tamil Nadu, India.

Received: 3 May. 2019, Revised: 2 Aug. 2019, Accepted: 12 Aug. 2019
Published online: 1 Sep. 2019

Abstract: Strontium doped Barium titanate nano powders were prepared by the wet chemical method using the starting materials barium chloride ($BaCl_2$), titanium dioxide (TiO_2), strontium carbonate ($SrCO_3$) and oxalic acid with high calcinations temperatures. The prepared nano powders were thermally grown onto well cleaned glass substrates under the vacuum of 10^{-5} torr, using 12A4 Hind Hivac coating unit. The X-ray diffraction patterns revealed that Sr doped $BaTiO_3$ nanoparticles possess tetragonal structure and the deposited films were polycrystalline in nature. Absorption coefficient, extinction coefficient, optical band gap and refractive index of films were estimated from optical transmittance spectrum. The extinction coefficient and refractive index of the $BaTiO_3$ thin films increases with increasing annealing temperature. The optical band gap energy value decreases with increase of annealing temperature.
Key words: barium titanate, Thermal evaporation, XRD, UV – Visible, Band gap.

1 Introduction

Large dielectric constant materials with perovskite structure have attracted great interest for potential applications in non-volatile, high speed ferroelectric random access memories (FeRAM) and dynamic random access memories (DRAM) in microwave devices especially like high speed microelectronics, radar, communication systems, humidity-sensitive sensors and electro-optical devices [1] because of their high dielectric constant, low leakage current density, and high dielectric breakdown strength. Such high dielectric constant ferroelectric thin films are $SrBi_2Ta_2O_9$ (SBT), $PbTiO_3$ (PTO), $PbZrTiO_3$ (PZT) and (Ba, Sr) TiO3; these materials are extensively studied for the above mentioned applications. Among these materials, Sr doped $BaTiO_3$ thin films are one of the most promising candidates. Sr doped $BaTiO_3$ thin films have been deposited by several methods sol–gel method [2, 3], chemical solution deposition [4], pulsed laser ablation [5] and radio-frequency (rf) sputtering [6]. Among the various methods, vacuum evaporation is an excellent method to produce thin films on various substrates with good stoichiometry that can easily be up scaled for industrial applications. Properties of thin films are dependent on various deposition parameters like deposition technique, annealing temperature, total pressure and composition of the operating gas. The annealing temperature plays a pivotal role in BTO thin film properties like orientation, crystallinity and surface morphology [7]. The function of Sr doped $BaTiO_3$ thin films in opto-electronic devices depends on structural and optical properties like grain size, lattice distortion, micro-strain, band gap, refractive index and absorption. It is important to study how these properties depend on deposition parameters. Several studies suggest that a strong correlation between the optical properties and the crystalline structure of the perovskite thin films exists. The band gap is the best example: with increasing crystallinity of the films the band gap decreases [8]. In this paper, we investigate Sr doped $BaTiO_3$ thin films prepared by vacuum evaporation and study their structural and optical properties and their surface morphology at various annealing temperature.

*Corresponding author: chandar.bellan@gmail.com

2 Experimental Details

2.1 Synthesis of Sr Doped $BaTiO_3$ Nanoparticles

Sr doped $BaTiO_3$ nanoparticles were synthesized by using wet chemical method. The starting materials used were barium chloride ($BaCl_2.2H_2O$, Aldrich Chemicals, purity 98%), titanium dioxide (TiO_2, Merck chemicals, purity 99%), strontium carbonate ($SrCO_3$, Merck chemicals, purity 99%) powder and oxalic acid (Merck chemicals, purity 99%). A solution of Ba: Ti: oxalic acid: $SrCO_3$ having mole ratio 1:1: 1: 0.1 was stirred and evaporated at 70 ˚C till a clear, viscous resin was obtained and then dried at 110 ˚C for 20h. The precursor formed was calcined at 900 ˚C for 2h using muffle furnace to form Sr doped $BaTiO_3$ nanoparticles.

2.2 Sr doped BaTiO3 Thin Film Preparation

The prepared nanopowders of Sr doped $BaTiO_3$ placed in the molybdenum boat (200 amps) and get heated with high current by energizing transformer. The transformer capable of supplying 150 amperes at 20 volts is used to provide the necessary current for heating the molybdenum source. Prior to evaporation, the evaporant material was carefully degassed at a lower temperature for about thirty minutes with the shutter closed. Deposition of the material on to pre-cleaned glass substrates under the pressure of about 10^{-5} Torr was achieved by slowly varying the current. A constant rate of evaporation 1Å/sec was maintained throughout the film preparation. The adhesion of the films to the substrate seems to be extremely good. The substrate to source distance was optimized to be at 0.175 m and source to crystal distance was optimized to be at 0.21 m inside the vacuum chamber. The as deposited thin films and annealed films at different temperatures for 1 h were used to study the structure, morphology and optical properties.

2.3 Measurements

Thickness of the films was measured through quartz crystal monitor (“Hind Hivac” Digital Thickness Monitor Model–DTM– 101). The structural aspects of the films wereanalyzed, using X-ray diffractometer with filtered CuKα radiation (λ = 1.5418 Å). The surface morphology of the films was examined by scanning electron microscope (SEM) and the high-resolution transmission electron microscopy (HRTEM). The optical studies were carried out by using JASCO – UV/VISIBLE spectrophotometer (JASCO V – 670, Japan).

3 Results and Discussion

3.1 Scanning Electron Microscope (SEM) Studies

Figure 1 shows the SEM images of Sr doped $BaTiO_3$ nano particles. Surface morphology of the nanoparticles revealed the presence of spherical and rod like grain structure distributed throughout the particles. Figure 2 (a, b, c) shows the SEM images of the Sr doped $BaTiO_3$ thin films at different annealing temperature. In all the films micro cracks were observed. These are attributed to the volume contraction during the crystallization process and the stress caused by the mismatch in thermal expansion coefficient between the film and substrate [9]. The grain size of the films increases with increasing annealing temperature, it could be attributed to higher grain growth at higher temperature.

3.2 Transmission Electron Microscope (TEM)

Figure 3 shows the HRTEM micrography of the Sr doped BaTiO3 nanoparticles with a well -isolated rod like morphology. The diameter of the rod is around 50 - 70 nm.

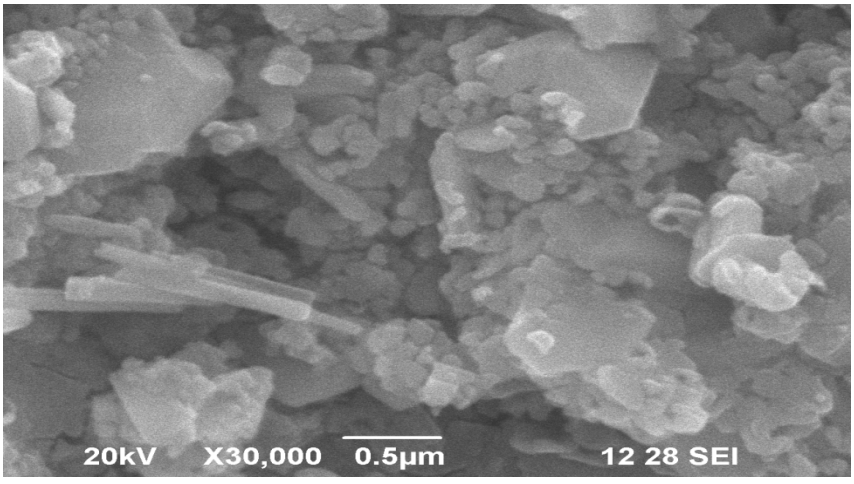

Fig.1: SEM images of Sr doped $BaTiO_3$ nanoparticles.

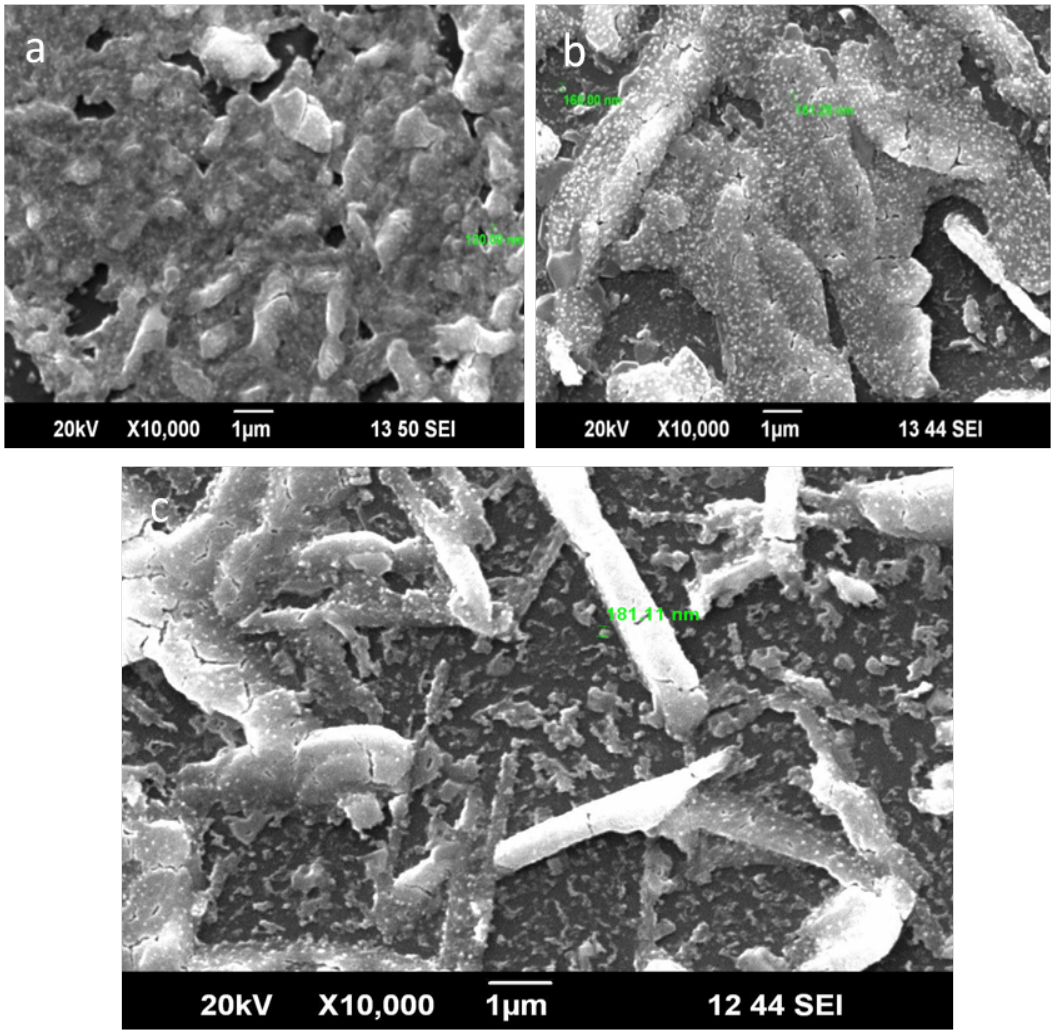

Fig.2: SEM images of Sr doped $BaTiO_3$ thin films of thickness 165 nm (a) as deposited (b) annealed at 473 K(c) annealed at 673 K.

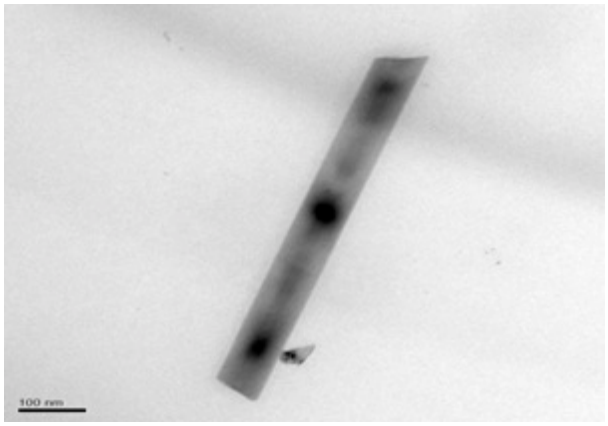

Fig.3: HRTEM micrography of the Sr doped BaTiO3 nanoparticles.

3.3 X – Ray Diffraction Analysis

Figure 4 shows the XRD pattern of Sr doped BaTiO3 nanoparticles calcined at 900 ˚C temperature for 2h. The peak splitting observed at an angle of 2θ = 44˚ to 46˚ indicated tetragonal structure. As the Sr is doped with BaTiO3, the cystallinity of the material increases where as the diffraction peaks shift towards higher angles as compared with the undoped BaTiO3 nanoparticles (10). This may be due to the decreased interatomic spacing and variation of lattice parameters by doping Sr with BaTiO3 nanoparticles [11, 12]. This effect can be explained by the fact that the ionic radius of Sr2+ (0.113 nm) is smaller than the ionic radius of Ba2+ (0.135 nm) [13, 14].

The crystallite size is calculated from the Scherrer's formula from the full with half – maximum (FWHM) of the XRD peaks

$$D = 0.94\lambda/\beta\cos\theta \quad (1)$$

Where λ is the wavelength of the X-rays used, 2θ is the angle between the incident and scattered X-rays and β is the full width at half maximum. The strain (ε) is calculated from the formula

$$\varepsilon = \beta\cos\theta/4 \quad (2)$$

The dislocation density (δ) is defined as the length of dislocation lines per unit volume of the crystal and is given by

$$\delta = 1/D^2 \quad (3)$$

The crystallite size was calculated at different diffraction angles and tabulated in the Table 1. From the Table it is observed that crystallite size is varies between 33 nm to 45 nm.

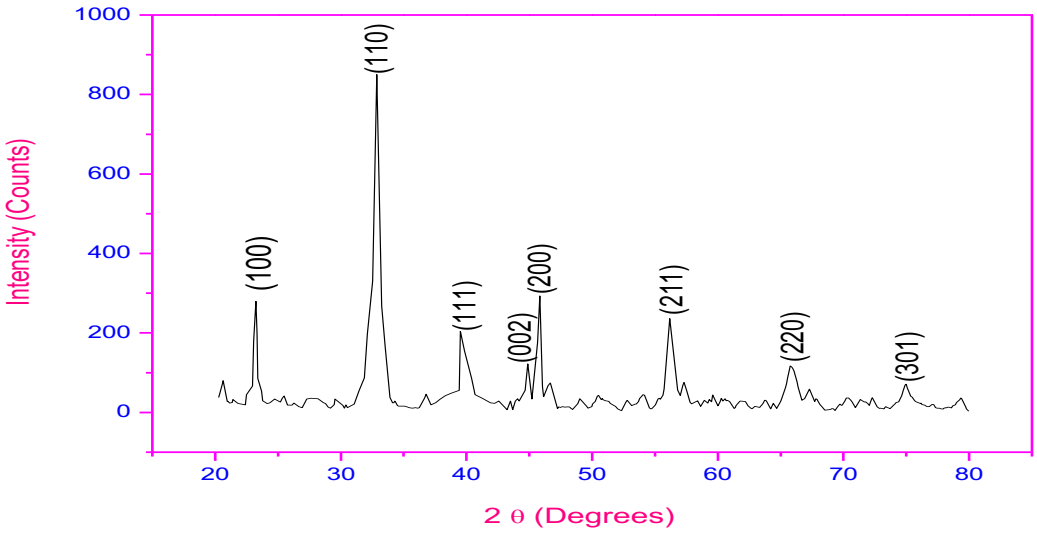

Fig.4: XRD pattern of Sr doped $BaTiO_3$ nanoparticles.

Table: 1 Structural parameter of Sr doped BaTiO3 nanoparticles.

Temperature (˚C)	Calculated values			Crystallite size
	2 θ (Degrees)	d (Å)	h k l	(nm)
900	23.67	3.756	100	36.45
	32.84	2.511	110	45.38
	39.67	2.27	111	35.43
	46.08	1.97	002	33.78
	56.057	1.639	211	42.53
	66.426	1.406	220	42.56
	74.95	1.266	301	43.34

3.4 Effect of Annealing Temperature on Sr Doped BaTiO3 Thin Films

Figure 5 shows the XRD pattern of Sr doped $BaTiO_3$ films of thickness 165 nm annealed at different temperatures. With the increase of annealing temperature, the peaks in the XRD pattern become sharper and more intense, indicating improved crystallinty. The XRD indicates the growth of the polycrystalline film with preferred orientation along the (110) plane for a different annealing temperatures. Similar behavior has also been reported by other researches for barium strontium titanate and $Ba_{0.64}Sr_{0.36}TiO_3$ films prepared by r.f. magnetron sputtering and sol - gel techniques [15, 16].

The crystallite size, strain and dislocation density of Sr doped $BaTiO_3$ thin films of thickness 165 nm annealed at different temperatures are presented in Table 2. From the table, it is seen that the crystallite size slightly increase with increase of annealing temperature, where as the strain and dislocation density decreases with increase of annealing temperature. The decrease in the strain and dislocation density indicates the formation of higher quality films with increase of annealing temperature.

Table 2: Structural parameters of Sr doped $BaTiO_3$ thin films of thickness 165 nm annealed at different temperatures.

Annealing temperature (˚C)	2θ (Degrees)	hkl	Crystallite size (D) (nm)	Strain (ε) x10^{-3} ($lin^{-2}m^4$)	Dislocation density (δ) x10^{15} (lin/m^2)
As deposited					
	24.08	100	25.86	1.340	1.495
	32.66	110	28.45	1.218	1.235
	39.01	111	23.13	1.498	1.869
	45.14	002	20.69	1.673	2.336
	56.61	112	27.87	1.393	1.616
200					
	24.08	100	27.28	1.270	1.342
	32.66	110	31.23	1.109	1.025
	39.01	111	25.57	1.355	1.529
	45.14	002	23.69	1.463	1.781
	56.61	112	31.07	1.115	1.035
400					
	24.08	100	30.42	1.137	1.080
	32.66	110	34.56	1.002	0.837
	39.01	111	28.68	1.208	1.215
	45.14	002	26.65	1.300	1.408
	56.61	112	33.58	1.032	0.886

3.5 Optical Studies

The transmittance spectra of Sr doped $BaTiO_3$ thin film of thicknesses 165 nm annealed at various temperatures is shown in figure 6. It is observed that the transmittance Decreases with increase in annealing temperatures. The Mobility of the atoms increases at higher temperatures causing the increase in crystallite size. The increase in crystallite size might be the reason of lower transmittance.

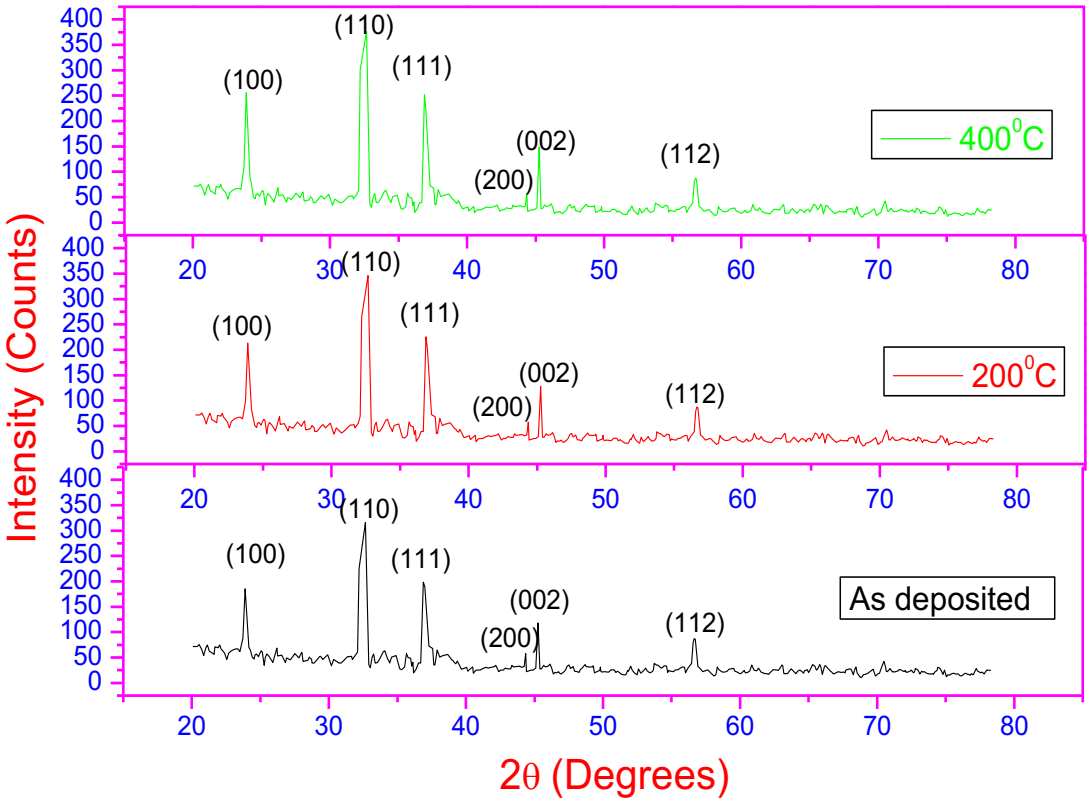

Fig. 5: XRD pattern of Sr doped $BaTiO_3$ films of thickness 165 nm annealed at different temperatures.

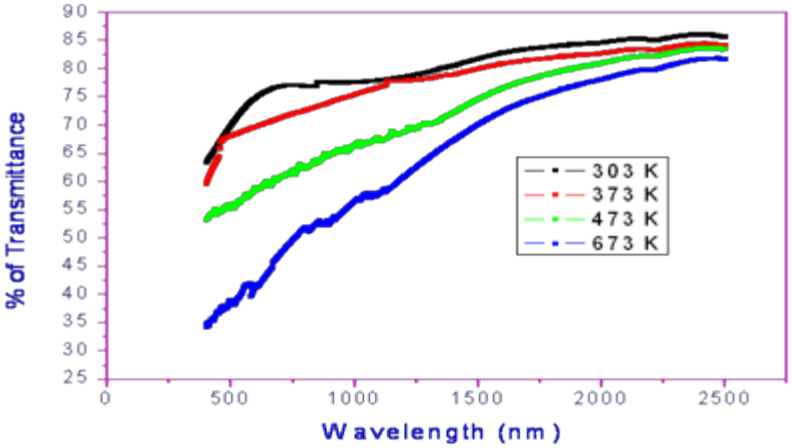

Fig. 6: Transmittance spectra of Sr doped $BaTiO_3$ thin film of thicknesses 165 nm annealed at various temperatures.

In order to describe the fundamental absorption edge, the spectral dependence of absorption coefficient (α) is directly determined using the relation,

$$\alpha = \frac{4\pi k_f}{\lambda} \qquad (4)$$

Where λ is the wavelength of the incident radiation and k_f is the extinction coefficient.

$$k_f = \frac{2.303 \log_{10}\left(\frac{1}{T}\right)\lambda}{4\pi t} \qquad (5)$$

Where't' is film thickness. The nature of transition can be investigated on the basis of dependence of α on the photon energy $h\upsilon$. For direct and allowed transitions, the theory of fundamental absorption leads to the following photon energy dependence near the absorption edge as,

$$\alpha \propto [h\upsilon - E_g]^m \quad (6)$$

Where $h\upsilon$ and E_g are the photon energy and the optical energy gap respectively. In this expression, the values of m are $\frac{1}{2}$ and 2 for direct and indirect transition respectively.

The optical properties of any material are characterized by two parameters n and k_f. The plot of transmission T against wavelength λ is found to vary as [17]

$$T = \frac{16n_a n_g n^2 \exp(-\alpha t)}{R_1^2 + R_2^2 \exp(-2\alpha t) + 2R_1 R_2 \exp(-\alpha t)\cos(4\pi nt/\lambda)} \quad (7)$$

Where,

$$R_1 = (n+n_a)(n_g+n)$$

$$R_2 = (n-n_a)(n_g-n)$$

α is the absorption coefficient and n, n_a, n_g are the Refractive indices of the film, air and substrate respectively. Iterations were carried out till the desired convergence was achieved.

The porosity (ρ) values (Volume of pores per volume of film) of the films were calculated using the relation [18]

$$\rho = 1 - \frac{n_f^2 - 1}{n_b^2 - 1} X100 \quad (8)$$

Figure 7 shows the variation of extinction coefficient with wavelength for Sr doped $BaTiO_3$ thin films of thickness 165 nm annealed at different temperatures. It is noted that the extinction coefficient of the film decreases with increase in annealing temperature.

thin films of thickness 165 nm annealed at different temperatures.

Figure 8 shows the variation of absorption coefficient (α) with wavelength of Sr doped $BaTiO_3$ thin films of thickness 165 nm at different annealing temperatures. From the absorption coefficient (α) the band gap energy of the films were calculated by using the equation (6).

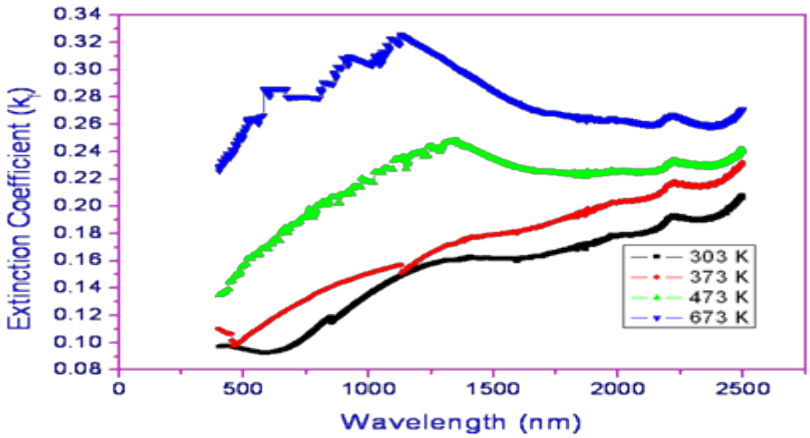

Fig.7: Variation of extinction coefficient with wavelength of Sr doped $BaTiO_3$ thin films of thickness 165 nm annealed at different temperatures.

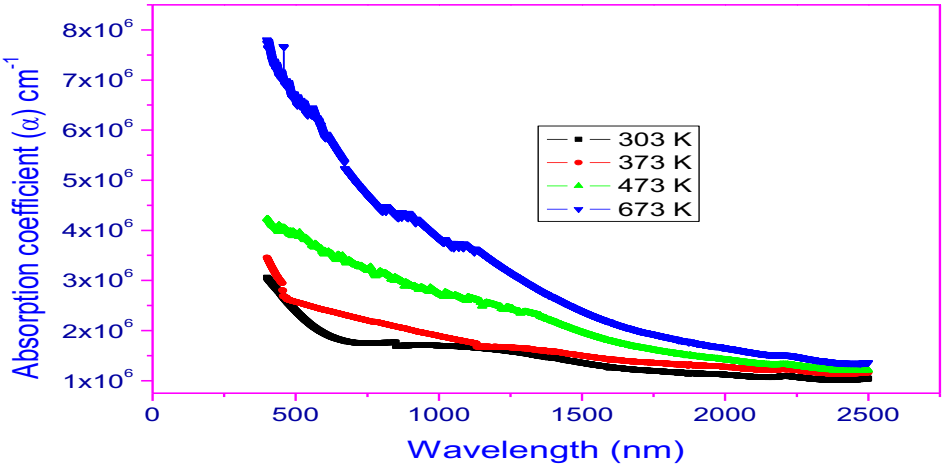

Fig.8: Variation of absorption coefficient (α) with wavelength of Sr doped $BaTiO_3$ thin films of thickness 150 nm at different annealing temperatures.

Figure 9. Shows the variation of $(\alpha h\upsilon)^2$ versus photon energy for Sr doped $BaTiO_3$ thin film of thickness 165 nm for different annealing temperature. The dependence of optical band gap with different annealing temperature is given in the Table 3. It is observed that direct band gap decreases with increase in the annealing temperatures. Band gap value obtained for the Sr doped $BaTiO_3$ films are higher than that reported by Cardona [19] for bulk $BaTiO_3$ and $SrTiO_3$ crystals (3.2 eV for both).
However, our results are in agreement with the band gap Values reported in the literature for $Ba_xSr_{1-x}TiO_3$ films for variable composition [20]. The shift in band gap of Sr doped $BaTiO_3$films to higher energies as compared to the bulk $BaTiO_3$ and $SrTiO_3$ crystals may be due to the stress – induced distortion band by lattice – film interaction. A combination of grain growth and partial strain relaxation in films are attributed to the reduction of energy gap with the increase of annealing temperature [21]. This behavior was similar to the behavior reported for annealed pure $BaTiO_3$ thin films (10).

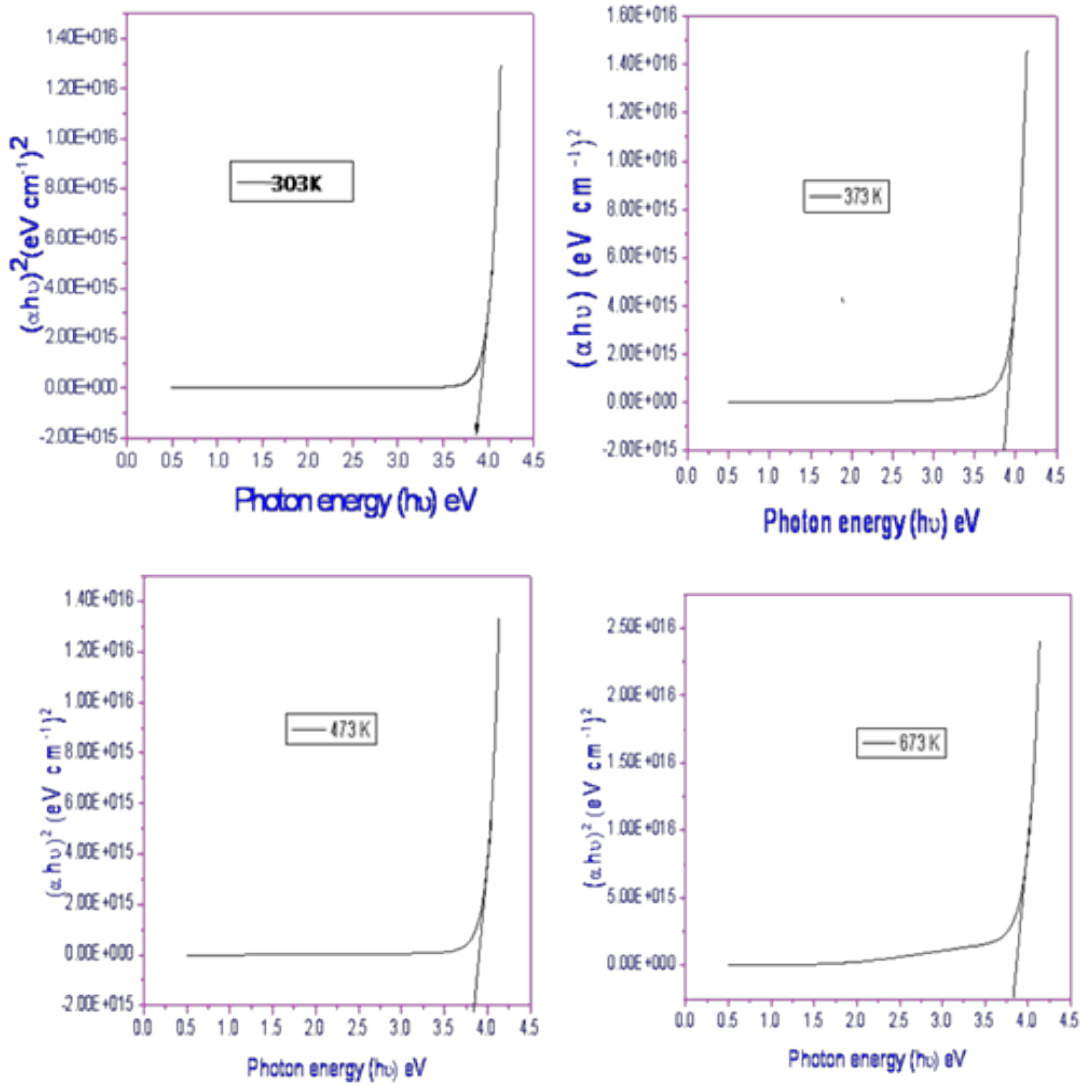

Fig.9: Plot $(\alpha h\upsilon)^2$ vs hυ for Sr doped $BaTiO_3$ films of various thicknesses.

Table 4 shows the porosity of the Sr doped $BaTiO_3$ thin film of thickness 165 nm annealed at different temperature. It is observed that porosity decreases with increase in annealing temperature (10).

Figure 10. Shows the refractive index with wavelength for Sr doped $BaTiO_3$ thin films of thickness 165 nm for different annealing temperatures. It is observed that refractive index of the $BaTiO_3$ thin film increases with annealing temperature. This is due reduction of porosity of

the films leading to an increase in the refractive index [22, 23]. This refractive index is higher than the refractive index of annealed pure $BaTiO_3$ thin films. It is due to decrease in porosity when compared to pure $BaTiO_3$ thin films (10).

Table 3: Band gap energy of Sr doped $BaTiO_3$ film of thickness 150 nm at different annealing temperatures.

Annealing temperature (K)	Band gap energy (eV)
303	3.88
373	3.85
473	3.84
673	3.82

Table 4: Porosity of the Sr doped $BaTiO_3$ thin film of thickness 165 nm annealed at different temperatures.

Temperature (K)	Porosity (ρ) %
303	40
373	30
473	23.6
673	9.4

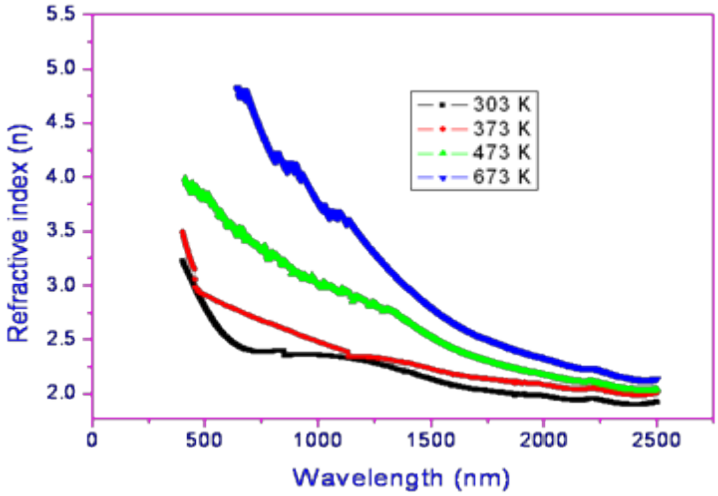

Fig.10: Variation of refractive index with wavelength for Sr doped $BaTiO_3$ thin films of thickness 165 nm for different annealing temperatures.

4 Conclusions

We have successfully prepared Sr doped $BaTiO_3$ nanopowders by wet chemical method using commercially available chemicals such as $BaCl_2$, TiO_2, $SrCO_3$ and oxalic acid. The prepared nanopowders were thermally grown onto well cleaned glass substrates by vacuum evaporation method. X-ray analysis showed that particle has a tetragonal nature and the deposited film has a polycrystalline nature. From the transmission spectra, the transmittance is found dependent on the annealing temperature. The transmittance decreases with annealing temperature. The value of extinction coefficient decreases with increases annealing temperature. The refractive index of the films increases with annealing temperature. The possible optical transition is direct-allowed type. The optical band gap energy shows an inverse dependence on annealing temperature.

References

[1] Y K Vayunandana Reddy, D Mergel, S Reuter, V Buck and M Sulkowski, J. Phys. D: Appl. Phys., **39**, 1161–1168, 2006.

[2] Sharma H B and Mansingh A 1998 J. Phys. D: Appl. Phys. 311527

[3] Hu Z, Wang G, Huang Z, Meng X and Chu J 2003 Semicond. Sci. Technol., **18**, 449, 2003.

[4] Petzelt J, Ostapchuk T, Paskin A and Rychetsky I 2003 J. Eur. Ceram. Soc., **23** 2627, 2003.
[5] P. Bhattacharya, T. Komeda, D. Park and Y. Nishioka, J. Appl. Phys., **32**, 4103, 1993.
[6] Jia Q X, Smith J L, Chang L H and Anderson W A 1998 Phil. Mag. B., **77**, 163, 1998.
[7] Zhang J, Cui D, Lu H, Chen Z, Zhou Y and Li L 1997 Japan. J. Appl. Phys., **36**, 276, 1997.
[8] Kamalasanan M N, Kumar N D and Chandra S 1994 J. Appl. Phys., **76**, 4603, 1994.
[9] C. B. Samantaray, A. Dhar, D. Bhattacharya, M. L. Mukherjee, S. K. Ray, J Mater Sci: Mater Electron., **12** 365 – 370, 2001.
[10] R. Sengodan B. Chandar Shekar, R. Balamurugan, R. Kannan, R. Ranjithkumar, , J. Optoelectron. Adv. Mater **(9–10)**, 595 – 603, 2017.
[11] V. Somani & S. M. Kalita, J. Electroceram.,**18**, 57 – 65, 2007.
[12] A. Wu, P. M. Vilarinho and M. Gonzalez, J Nanopart Res., **12**, 2221 – 2231, 2010.
[13] A. J. Moulson and J. M. Herbert, Electroceramics: Materials, properties and Applications, 2nd edition, Wiley, New York., 2003.
[14] J. Ravez, A. Simon, J. Solid State Chemistry., **162** , 260, 2001.
[15] C. B. Samantaray, A. Dhar, D. Bhattacharya, M. L. Mukherjee and S. K. Ray, J Mater Sci: Mater Electron., **12**, 365 – 370, 2001.
[16] L. Dong, R. Yue, L. Liu, X. Wang, J. Liu and T. Ren, Int J Infrared Millimeter Waves., **24(8),** 1341- 1349, 2003.
[17] D.K. Schroder, "Semiconductor Material Device Characterization," 2nd edn. (Wiley, New York, 1998).
[18] R.M. Rose, L.A. Shepard and J. Wulff, "The Structure and Properties of Materials", (John Wiley and Sons Inc., New York, 1967)., **4**, 1967.
[19] M. Cardona, phys. Rev. A., **140,** 651, 1965.
[20] L. D. Rotter, M. D. Vaudin, J. E. Bonevich, D. L. Kaiser and S. O. Park, Thin solid films., 368, 41, 2000.
[21] G. M. Davics and M. C. Gower, Appl. Phys. Lett., **55** 112, 1989.
[22] R. Thomas, D. C. Dube, M. N. Kamalasanan and S. Chandra, Thin solid films., **346**, 212, 1999.
[23] L.V. Mahneeshya, V. S. Anitha, S. S. Lekshmy, L. John Berlin, P. B. Nair, G. P. Daniel, P. V. Thomas and K. Joy, J Mater Sci: Mater Electron., **24**, 848-854, 2013.